crystals

MDPI

Article

Synthesis of *N*-(Anthracen-9-ylmethyl)-*N*-methyl-2-(phenylsulfonyl)ethanamine via Microwave Green Synthesis Method: X-ray Characterization, DFT and Hirshfeld Analysis

Mohyeddine Al-Qubati [1,2], Hazem A. Ghabbour [3], Saied M. Soliman [4], Abdullah Mohammed Al-Majid [5], Assem Barakat [5,*] and Mujeeb A. Sultan [6,*]

1 Department of physics, Faculty of Applied Sciences, Taiz University, Taiz 6803, Yemen; mohyeddine@just.ac
2 Faculty of Engineering and Information Technology, Aljanad University for Science and Technology, Taiz 6934, Yemen
3 Department of Medicinal Chemistry, Faculty of Pharmacy, University of Mansoura, Mansoura 35516, Egypt; hghabbour@mans.edu.eg
4 Department of Chemistry, Faculty of Science, Alexandria University, P.O. Box 426, Ibrahimia, Alexandria 21321, Egypt; saied1soliman@yahoo.com or saeed.soliman@alexu.edu.eg
5 Department of Chemistry, College of Science, King Saud University, P.O. Box 2455, Riyadh 11451, Saudi Arabia; amajid@ksu.edu.sa
6 Department of Pharmacy, Faculty of Medical Sciences, Aljanad University for Science and Technology, Taiz 6934, Yemen
* Correspondence: ambarakat@ksu.edu.sa (A.B.); mujeeb.AA@just.ac (M.A.S.); Tel.: +966-11467-5901 (A.B.); +967-77587-3672 (M.A.S.); Fax: +966-11467-5992 (A.B.)

Received: 2 July 2020; Accepted: 23 July 2020; Published: 26 July 2020

Abstract: *N*-(Anthracen-9-ylmethyl)-*N*-methyl-2-(phenylsulfonyl)ethanamine **3** has been synthesized via the aza-Michael addition approach by reaction of the corresponding amine with the vinyl sulfone derivative under microwave conditions. The structure of the aza-Michael product **3** is elucidated by X-ray crystallography. The study of molecular packing by employing the Hirshfeld analysis indicates that the percentages of O . . . H, C . . . H and H . . . H contacts are 16.8%, 34.1% and 48.6%, respectively, where the O...H hydrogen bonds have the characteristics of short and strong contacts while the C...H contacts are considered weak. Density functional theory (DFT) investigations show that the aza-Michael product **3** is polar with a net dipole moment of 5.2315 debye.

Keywords: anthracene; aza-Michael addition; microwave; Hirshfeld analysis; DFT

1. Introduction

Anthracenes, in particular crystalline materials, have attracted attention due to their wide energy gaps, high fluorescence quantum yields, high thermal stability and consequently their promising applications as organic semiconductors for organic field-effect transistors (OFETs) and organic light-emitting diodes (OLEDs) [1–7].

The atom-efficient transformation toward the synthesis of bulk molecules from smaller starting materials is desirable in organic synthesis [8–10]. The formation of carbon–nitrogen bonds is one of the most important synthetic approaches in modern organic chemistry. Specifically, the aza-Michael addition that was discovered in 1874 is considered one of the most efficient protocols for C–N formation where the amine acts as a Michael donor and the olefin acts as a Michael acceptor to provide an aza-Michael adduct [11,12]. Most classical aza-Michael reactions are usually activated by a strong base or acid, but ultrasound or microwave assisted reactions have been reported as efficient and cleaner

methods for aza-Michael addition [13,14]. Furthermore, the aza-Michael addition was proved to proceed using the Lewis acid catalyzed reaction [15,16] and ionic liquids [17]. The reaction also proceeded as either an intermolecular or intramolecular addition [18] and under eco-friendly conditions [19].

α,β-unsaturated sulfonyl derivatives were used as labelling reagents due to their highly electrophilic nature [20–22]. Vinyl sulfones are an alternative class of thiol alkylating reagents to maleimides which have been used in a variety of bioconjugation reactions [23]. In particular, phenyl vinyl sulfone has been employed in different transformations, for example exploited as dienophile in [4+2] Diels-Alder cycloaddition reactions [24–27]. Indeed, vinyl sulfones have been explored as Michael acceptors with a range of nucleophiles to afford an aza-Michael adduct [28,29]. Among the aza-Michael addition protocols, the vinyl sulfones were utilized as a Michael acceptor for the synthesis of interesting scaffolds in the presence of catalysts such as a palladium complex or a copper salt. The latter is easy to handle, safe and cheap [30].

Along these lines, here we report the synthesis of an aza-Michael product, namely; *N*-(anthracen-9-ylmethyl)-*N*-methyl-2-(phenylsulfonyl)ethanamine **3** via reaction of 1-(anthracen-9-yl)-*N*-methylmethanamine **1** as a Michael donor with phenyl vinyl sulfone as the Michael acceptor. The X-ray crystallography, Hirshfeld analysis and DFT studies were investigated to explore the structure and electronic aspects of this aza-Michael product **3**.

2. Materials and Methods

2.1. General Notes

The starting material 1-(anthracen-9-yl)-*N*-methylmethanamine 1 was purchased from Aldrich Chemical Co. (now Merk). The reaction was monitored by thin-layer chromatography (TLC) on pre-coated silica gel plates from Merck (Germany) using solvent system 4: 1 DCM: PE and the spots were visualized with a 254 nm UV lamp. JEOL 400 MHz NMR spectrometer (JEOL, Japan) was utilized to obtain ^{1}H-NMR spectra of the aza-Michael product 3.

2.2. Synthesis of N-(anthracen-9-ylmethyl)-N-methyl-2-(phenylsulfonyl)ethanamine **3**

To an oven-dried 10 mL microwave vessel containing a stir bar, a solution of 1-(anthracen-9-yl)-*N*-methylmethanamine **1** (50 mg, mmol) and phenyl vinyl sulfone **2** (50 mg, mmol) in xylene (3 mL) was added. After sealing this vessel with a plastic microwave septum, the mixture was irradiated utilizing microwave under the following conditions: 250 W, 250 psi, at 150 °C for 20 h. The reaction was monitored by TLC and after the reaction was completed, the mixture was cooled down and the excess solvent was removed using a rotary evaporator to afford the aza-Michael compound **3** as a clean product. For further purification, a mixture was chromatographed on silica gel using 4: 1 DCM: PE. ^{1}H-NMR ($CDCl_3$, JEOL 400 MHz): δ = 2.21, (s, 3H), 2.90 (t, J = 7.2, 2H), 3.25 (t, J = 7.2, 2H), 4.38 (s, 2H), 7.31 (t, J = 8, 2H), 7.41–7.51 (m, 5H), 7.66 (d, J = 8, 2H), 7.95 (d, J = 8, 2H), 8.28–8.36 (m, 3H).

2.3. X-ray Crystallography Analysis

A suitable single crystal for the aza-Michael product **3** was obtained by a slow evaporation technique for the solution of the compound in xylene at rt. The Bruker APEX-II D8 Venture diffractometer was employed for data collection. Data reduction and cell refinement were carried out by Bruker SAINT. SHELXT [31,32] was used to solve structure. CCDC 1825185 contained all crystallographic data of the aza-Michael product **3** where the full-matrix least-squares techniques with anisotropic thermal data for nonhydrogen atoms on F^2 were employed for the final refinement of the structure.

2.4. Hirshfeld Surface Analysis

The intermolecular interactions in the crystal structure of the aza-Michael product **3** were explored by topology analyses using the Crystal Explorer 17.5 program [33,34].

2.5. Computational Methods

Gaussian 09 software package was used for all DFT study [35]. B3LYP/6-31G(d,p) protocol was employed for the molecular geometry optimization of the aza-Michael product **3**. In addition, natural charges were calculated using the Gaussian 09 built in NBO 3.1 [36] program at the optimized geometry of the aza-Michael product **3**.

3. Results and Discussion

3.1. Synthesis

As a part of our ongoing interest in the strategies of atom economy synthesis starting from simple, cheap and commercially available materials, we report the synthesis of aza-Michael product **3** from the reaction of 1-(anthracen-9-yl)-N-methylmethanamine **1** with α,β-unsaturated olefin; phenyl vinyl sulfone **2,** Scheme 1. The reaction was successfully carried out under microwave conditions. The ^{1}H NMR spectrum showed the main characteristic protons of the synthesized compound. A singlet peak at δ 2.21 ppm was assigned for the methyl group while the two triplet peaks at δ 2.90, and 3.25 ppm with J = 7.2Hz were assigned for the two CH_2 protons. Additionally, a singlet peak at δ 4.38 was assigned for the methine group. Finally, the signals observed in the range of δ 7.31–8.36 ppm were characteristics for the aromatic protons.

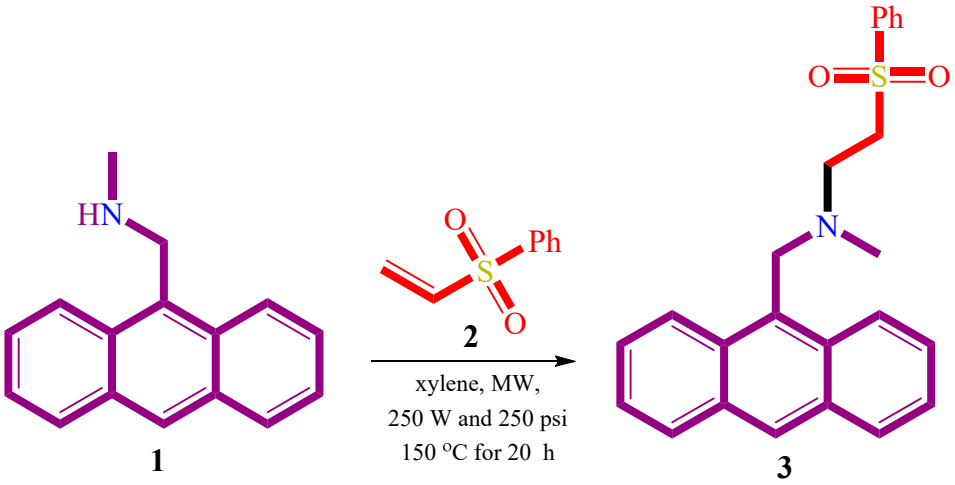

Scheme 1. Synthesis of aza-Michael product **3**.

3.2. Crystal Data

The crystallographic data and refinement information of aza-Michael product **3**, $C_{24}H_{23}NO_2S$, are presented in Table 1. Selected bond angles and bond lengths are listed in Table 2 while the observed X-ray structure is given in Figure 1. The compound crystallized in the Monoclinic crystal system and $P2_1$ space group with one molecule in the asymmetric formula and $Z = 2$. All bond angles as well as bond lengths are in normal ranges [34].

Table 1. Experimental details of aza-Michael product **3**.

Crystal Data	
Chemical formula	$C_{24}H_{23}NO_2S$
M_{Wt}	389.49
Crystal system, space group	Monoclinic, $P2_1$
Temperature (K)	293

Table 1. *Cont.*

Crystal Data	
a, *b*, *c* (Å)	5.6755 (6), 14.7098 (16), 12.0407 (13)
β (°)	94.139 (4)
V (Å^3)	1002.60 (19)
Z	2
Radiation type	Mo *Kα*
μ (mm $^{-1}$)	0.18
Crystal size (mm)	0.44 × 0.21 × 0.15
Data Collection	
Diffractometer	Bruker APEX-II D8 venture diffractometer
Absorption correction	Multi-scan SADABS Bruker 2014
T_{min}, T_{max}	0.867, 0.901
Number of measured, independent and observed [I > 2σ(I)] reflections	15116, 4588, 2912
R_{int}	0.100
Refinement	
R[F^2 > 2σ(F^2)], wR(F^2), S	0.062, 0.152, 0.94
Number of reflections	4588
Number of parameters	253
Number of restraints	1
H-atom treatment	H-atom parameters constrained
$\Delta\rho_{max}$, $\Delta\rho_{min}$ (e Å^{-3})	0.21, −0.33

Table 2. Selected geometric parameters (Å, °).

S1—O1	1.441 (4)	N1—C15	1.478 (6)
S1—O2	1.432 (4)	N1—C16	1.459 (6)
S1—C18	1.765 (5)	N1—C17	1.450 (6)
S1—C19	1.762 (6)		
O1—S1—O2	118.5 (2)	C15—N1—C17	110.2 (3)
O1—S1—C18	107.5 (2)	C16—N1—C17	110.5 (3)
O1—S1—C19	108.2 (2)	N1—C15—C14	111.1 (4)
O2—S1—C18	109.4 (2)	N1—C17—C18	111.1 (4)
O2—S1—C19	107.7 (2)	S1—C18—C17	113.4 (3)
C18—S1—C19	104.8 (2)	S1—C19—C20	121.1 (4)
C15—N1—C16	110.7 (4)	S1—C19—C24	118.3 (4)

In Figure 2, the molecule of **3** is linked with neighboring molecular units *via* two non-classical intermolecular C-H...O interactions as well as two C-H...π contacts (Table 3). The three dimensional molecular packing structure of **3** showing the molecules are connected by the C-H...O and C-H...π interactions are given in Figure 3.

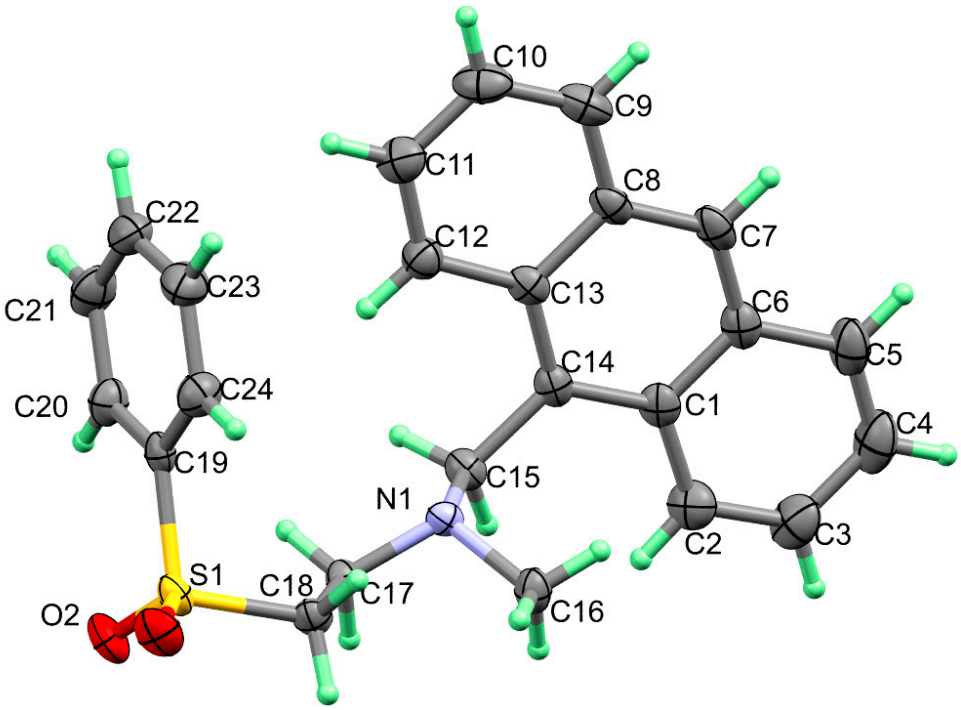

Figure 1. X-ray structure with thermal displacement ellipsoids plotted at 30% probability level for molecule **3**.

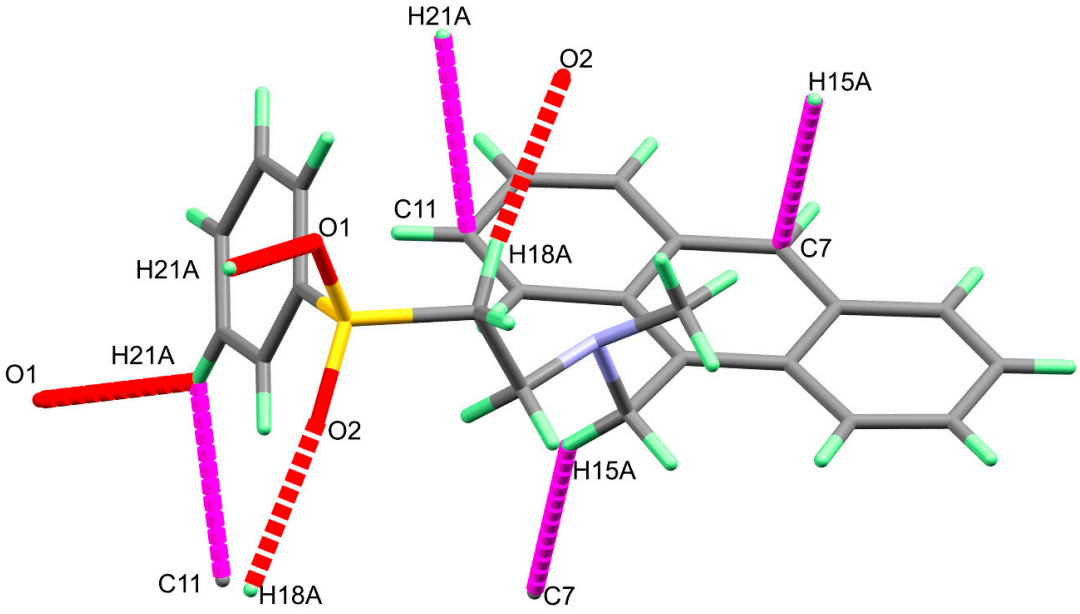

Figure 2. The intermolecular C-H...π (magenta) and O...H (red) contacts in the crystal structure of **3**.

Table 3. Intermolecular contacts (Å, °) observed in the crystal structure of molecule **3**.

D—H···A	D—H	H···A	D···A	D—H···A
C18—H18A···O2^{i}	0.97	2.41	3.347 (6)	161.0
C21-H21A … O1^{ii}	0.931	2.639	3.379(8)	136.9
C15-H15A … C7i	0.971	2.867	3.621(7)	135.2
C21-H21A … C11^{i}	0.931	2.84	3.639(9)	144.7
(i) *x* − 1, *y*, *z*; *(ii)* 2−*x*,−1/2+*y*, −*z*				

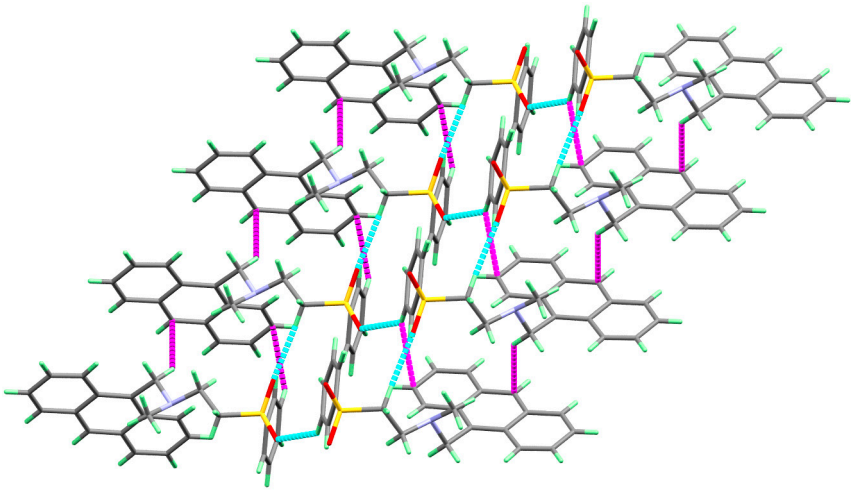

Figure 3. Molecular packing of molecule **3** via C-H...π (magenta) and O...H (red) interactions.

3.3. Analysis of Molecular Packing

Hirshfeld surfaces mapped over d_{norm}, shape index (SI) and curvedness for aza-Michael product **3** are shown in Figure 4. Summary of the most important contacts and their percentages are shown in Figure 5. The Hirshfeld d_{norm} maps of aza-Michael product **3** showed that the molecular units are mainly packed by many O...H polar short contacts which are significantly more important than the weak H...H and C...H interactions. The percentages of the O … H, C … H and H … H contacts are 16.8%, 34.1% and 48.6%, respectively. It is clear that the strong O … H contacts appeared as intense red regions in d_{norm} and sharp spikes in the fingerprint plot (Figure 6a) while the weak C … H contacts appeared as fad red regions in d_{norm} and broad peaks in the fingerprint plot (Figure 6b). The shortest O...H contact distances are O2...H18A (2.308 Å) and O1...H21A (2.530 Å) which are significantly shorter than the van der Waals radii sum of the two elements (2.61 Å). In contrast, the weak C11 … H21A (2.716 Å) and C7 … H15A (2.789 Å) contacts which belong to the C-H … π interactions have slightly shorter intermolecular distances compared to the van der Waals radii sum of the two elements (2.79 Å). The shape index and curvedness maps revealed the absence of significant ring π-π stacking interactions.

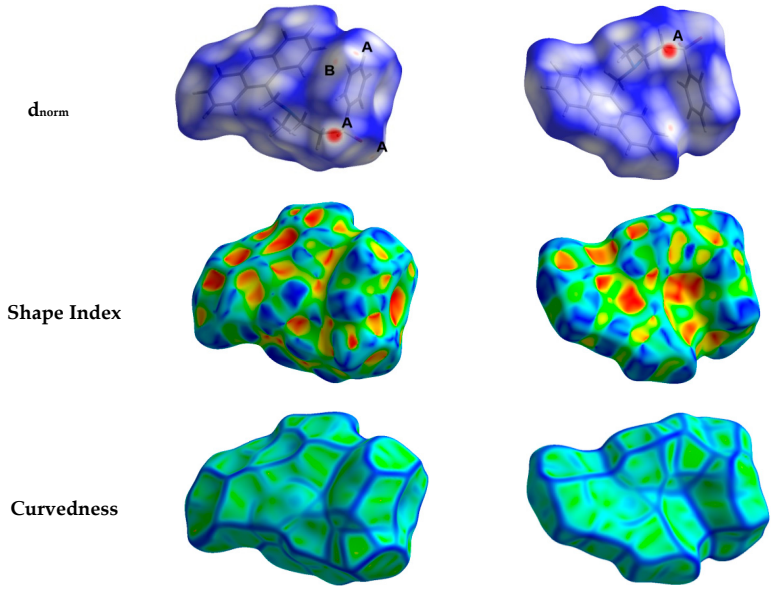

Figure 4. Hirshfeld surfaces mapped over d_{norm}, curvedness and shape index for aza-Michael product **3**. Regions A and B in the d_{norm} maps refer to the strong and weak O … H and C … H contacts, respectively.

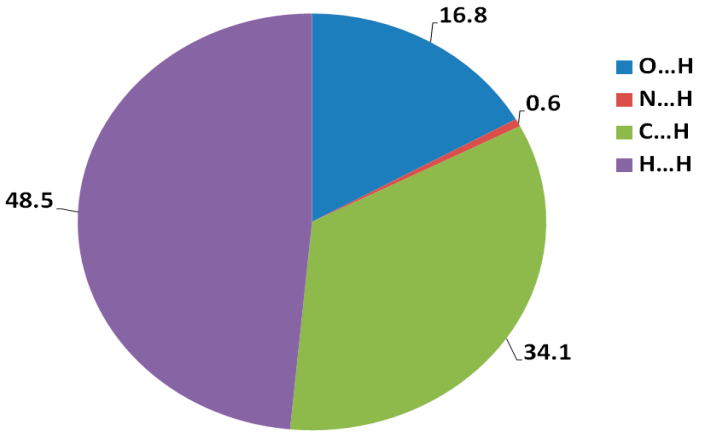

Figure 5. Percentages of the intermolecular interactions in the aza-Michael product **3** crystal structure.

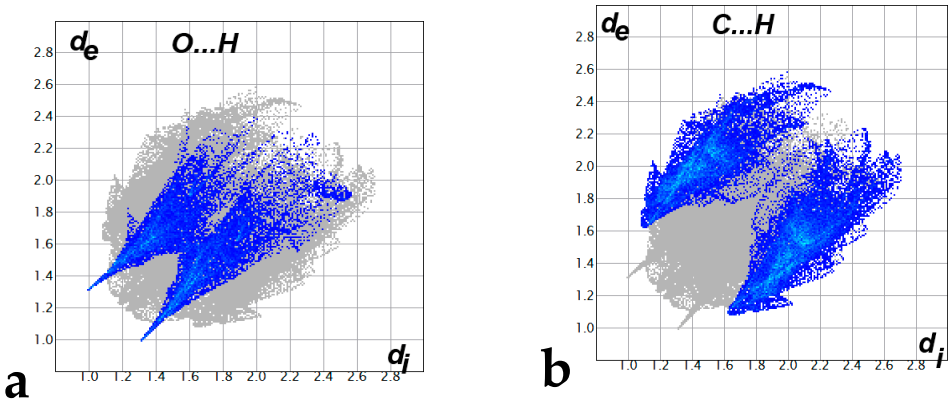

Figure 6. The decomposed fingerprint plots of the strong O...H (**a**) and weak C . . . H (**b**) contacts.

3.4. Geometric Parameters

The crystal structure of **3** was set to relax in the gas phase and the optimized structure is presented in Figure 7. The computed bond angles and distances are listed in (Table S1, Supplementary Data). It has been observed that there is very good agreement between the calculated bond distances and the experimental values with a high correlation coefficient (R^2) of 0.918 (Figure 8).

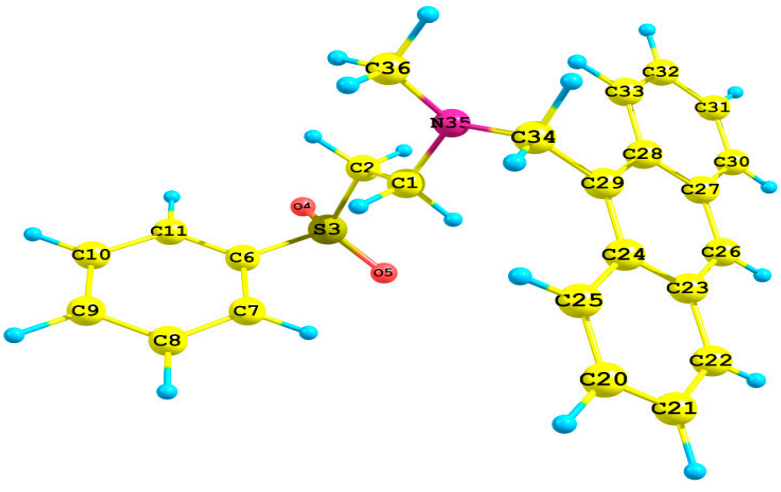

Figure 7. The optimized molecular structure of aza-Michael product **3**.

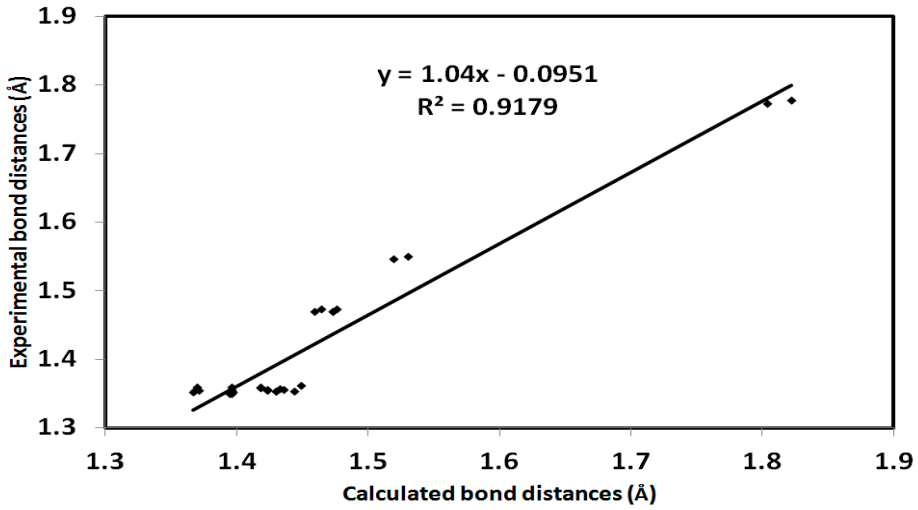

Figure 8. Correlation diagram of the computed bond distances and the experimental values of aza-Michael product **3**. The correlation coefficient for bond angles is 0.835.

Table 3 is summarized in Table 4. The oxygen (O), nitrogen (N) and carbon (C) atoms have negative charge densities, where the O (−0.9534 to −0.9554 e) and N (−0.5047 e) atoms have the most negative charge density. In contrast, the Sulphur (S) atom has the most positive charge of 2.2117 e. The electron density mapped over molecular electrostatic potential (MEP) strongly indicated the varied charge distributions which are responsible for the polarity of the compound. The computed dipole moment is 5.2315 debye and the vector showing the net direction of the dipole is depicted in Figure 9. In addition, the MEP map revealed that the oxygen atoms are the most favored atomic sites for hydrogen bonding interactions as the hydrogen bond acceptor.

Table 4. The calculated natural charges at atomic sites of aza-Michael product **3** [a].

Atom	Charge	Atom	Charge	Atom	Charge	Atom	Charge
C1	−0.2892	C27	−0.0540	H14	0.2860	H40	0.2323
C2	−0.7026	C28	−0.0398	H15	0.2711	H41	0.2353
S3	2.2117	C29	−0.0128	H16	0.2480	H42	0.2376
O4	−0.9534	C30	−0.2064	H17	0.2460	H43	0.2412
O5	−0.9554	C31	−0.2370	H18	0.2481	H44	0.2401
C6	−0.3292	C32	−0.2321	H19	0.2662	H45	0.2477
C7	−0.2206	C33	−0.2143	C20	−0.2314	H46	0.2115
C8	−0.2321	C34	−0.2781	C21	−0.2401	H47	0.2477
C9	−0.2175	N35	−0.5047	C22	−0.2019	H48	0.2572
C10	−0.2321	C36	−0.4830	C23	−0.0545	H49	0.2284
C11	−0.2196	H37	0.2395	C24	−0.0444	H50	0.1959
H12	0.2681	H38	0.2415	C25	−0.2198	H51	0.2329
H13	0.2077	H39	0.2381	C26	−0.1735	–	–

[a] Atom numbering (refer to Figure 7).

On other hand, the highest occupied (HOMO) and lowest unoccupied (LUMO) molecular orbitals of the studied system are shown in Figure 9. The HOMO (−5.247 eV) and LUMO (−1.734 eV) orbitals are mainly distributed over the π-system of the anthracene moiety. The HOMO of the compound is extended over the nitrogen heteroatom indicating a HOMO→LUMO transition of mixed n-π* and π-π* excitations. The energy of this electronic transition is 3.513 eV.

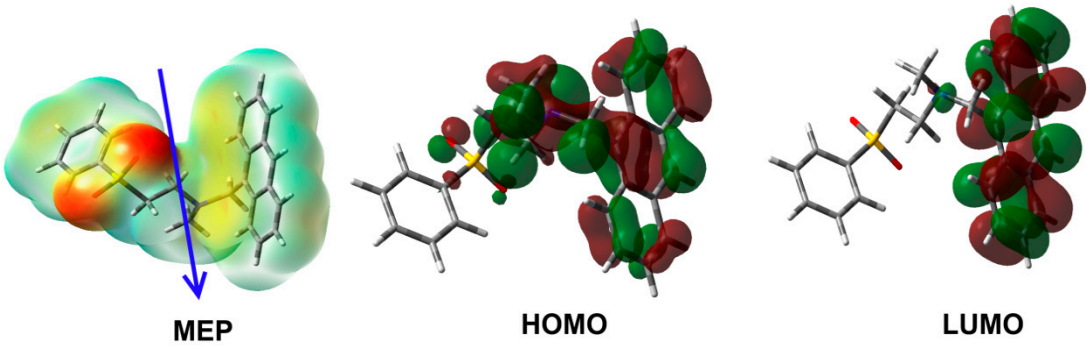

Figure 9. MEP, HOMO and LUMO of aza-Michael product **3.**

4. Conclusions

We conclude that aza-Michael product **3**, namely *N*-(anthracen-9-ylmethyl)-*N*-methyl-2-(phenylsulfonyl) ethanamine as a Michael donor **1** successfully reacted with phenyl vinyl sulfone as a Michael acceptor **2** in xylene under microwave conditions to afford aza-Michael product **3**. This aza-Michael product **3** was structurally elucidated using an X-ray technique. Analysis of molecular packing has been performed using Hirshfeld calculations and results indicate that polar O . . . H hydrogen bonds are more important than weak C-H...π interactions in the molecular packing. The charge distribution and the polarity of the aza-Michael product **3** were predicted using DFT calculations.

Supplementary Materials: The following are available online at http://www.mdpi.com/2073-4352/10/8/643/s1; Table S1: The calculated bond distances and angles compared to the experimental data of aza-Michael product **3** [a].

Author Contributions: Conceptualization, M.A.S. and A.B.; methodology, M.A.S.; software, A.B., S.M.S. and H.A.G.; validation, M.A.-Q., A.B. and M.A.S.; formal analysis, M.A.S.; investigation, M.A.-Q.; A.M.A.-M.; H.A.G. and S.M.S.; resources, M.A.-Q.; A.M.A.-M.; data curation, M.A.-Q., A.B. and M.A.S.; writing—original draft preparation, A.B. and M.A.S.; writing—review and editing, S.M.S., H.A.G., A.B. and M.A.S.; visualization S.M.S., H.A.G., A.B. and M.A.S.; supervision, M.A.-Q. and A.M.A.-M.; project administration, A.B.; funding acquisition, A.B. and M.A.S. All authors have read and agreed to the published version of the manuscript.

Funding: King Saud University-Researchers Supporting Project Number (RSP-2020/64).

Acknowledgments: The authors would like to extend their sincere appreciation to Researchers Supporting Project Number (RSP-2020/64), King Saud University, Riyadh, Saudi Arabia. M.A and M.A.S thank Aljanad University of Science and Technology, Taiz, Republic of Yemen for facilities access.

Conflicts of Interest: The authors declare no conflict of interest.

References

1. Jones, K. Anthracene and Anthracene-Tetracene Crystals from Vapor. *Mol. Cryst. Liq. Cryst.* **1968**, *3*, 393–396. [CrossRef]
2. Jung, H.; Lee, H.; Kang, S.; Shin, D.; Park, M.; Kay, K.-Y.; Park, J. Synthesis and electroluminescent properties of new blue emitters based on dual anthracene and dibenzo-diazocine moieties. *Mol. Cryst. Liq. Cryst.* **2017**, *659*, 140–146. [CrossRef]
3. Jung, H.; Lee, H.; Kang, S.; Shin, D.-H.; Kay, K.-Y.; Park, J. New anthracene derivatives containing coumarin moiety for organic light-emitting diodes. *Mol. Cryst. Liq. Cryst.* **2017**, *654*, 90–95. [CrossRef]
4. Kay, K.-Y.; Kim, J.; Cho, H.; Park, J.-W. Synthesis and electroluminescent properties of fluorene-and anthracene-derivatives containing novel tetraphenylbenzene moiety. *Mol. Cryst. Liq. Cryst.* **2004**, *424*, 167–172. [CrossRef]
5. Kim, S.H.; Kim, J.; Lee, S.E.; Kim, Y.K.; Yoon, S.S. Electroluminescent properties of naphthalene end-capping bis-anthracene derivatives. *Mol. Cryst. Liq. Cryst.* **2016**, *636*, 30–37. [CrossRef]
6. Lee, H.; Kang, S.; Ann, C.; Shin, D.; Park, M.; Kay, K.-Y.; Park, J. New anthracene derivatives including diazocine for blue emitting materials. *Mol. Cryst. Liq. Cryst.* **2017**, *651*, 71–76. [CrossRef]

7. Mack, M.; Eisenbach, C. Photochromic effects of an anthracene derivative in polyurethane. *Mol. Cryst. Liq. Cryst.* **2005**, *431*, 397–402. [CrossRef]
8. Elassar, A.-Z.A.; El-Khair, A.A. Recent developments in the chemistry of enaminones. *Tetrahedron* **2003**, *59*, 8463–8480. [CrossRef]
9. Gomha, S.M.; Abdel-Aziz, H.A. Enaminones as Building Blocks in Heterocyclic Preparations: Synthesis of Novel Pyrazoles, Pyrazolo-[3, 4-d] pyridazines, Pyrazolo [1, 5-a] pyrimidines, Pyrido-[2, 3-d] pyrimidines Linked to Imidazo [2, 1-a] thiazole System. *Heterocycles* **2012**, *85*, 2291. [CrossRef]
10. Shetty, S.; Kalluraya, B. Enaminones as building blocks: Synthesis of novel substituted pyrazoles as possible antioxidants. *Indian J. Chem.* **2016**, *55B*, 501–506.
11. Genest, A.; Portinha, D.; Fleury, E.; Ganachaud, F. The aza-Michael reaction as an alternative strategy to generate advanced silicon-based (macro) molecules and materials. *Prog. Polym. Sci.* **2017**, *72*, 61–110. [CrossRef]
12. Rulev, A.Y. Aza-Michael reaction: Achievements and prospects. *Russ. Chem. Rev.* **2011**, *80*, 197. [CrossRef]
13. Labade, V.B.; Pawar, S.S.; Shingare, M.S. Cesium fluoride catalyzed Aza-Michael addition reaction in aqueous media. *Mon. Für Chem. Chem. Mon.* **2011**, *142*, 1055. [CrossRef]
14. Wei, T.-B.; Hua, M.-T.; Shi, H.-X.; Liu, Y.; Zhang, Y.-M. Aza-Michael addition of acrylonitrile with 2-aryloxymethylbenzimidazole derivatives under microwave irradiation. *J. Chem. Res.* **2010**, *34*, 452. [CrossRef]
15. Azizi, N.; Saidi, M.R. LiClO4 accelerated Michael addition of amines to α, β-unsaturated olefins under solvent-free conditions. *Tetrahedron* **2004**, *60*, 383–387. [CrossRef]
16. Xu, L.W.; Li, L.; Xia, C.G. Transition-metal-based Lewis acid catalysis of Aza-type Michael additions of amines to α, β-unsaturated electrophiles in water. *Helv. Chim. Acta* **2004**, *87*, 1522–1526. [CrossRef]
17. Ying, A.-G.; Liu, L.; Wu, G.-F.; Chen, G.; Chen, X.-Z.; Ye, W.-D. Aza-Michael addition of aliphatic or aromatic amines to α, β-unsaturated compounds catalyzed by a DBU-derived ionic liquid under solvent-free conditions. *Tetrahedron Lett.* **2009**, *50*, 1653–1657. [CrossRef]
18. Le Guen, C.; Tran Do, M.-L.; Chardon, A.; Lebargy, C.; Lohier, J.-F.o.; Pfund, E.; Lequeux, T. Access to fluoropyrrolidines by intramolecular aza-Michael addition reaction. *J. Org. Chem.* **2016**, *81*, 6714–6720. [CrossRef]
19. Bosica, G.; Debono, A.J. Uncatalyzed, green aza-Michael addition of amines to dimethyl maleate. *Tetrahedron* **2014**, *70*, 6607–6612. [CrossRef]
20. Morales-Sanfrutos, J.; Megia-Fernandez, A.; Hernandez-Mateo, F.; Giron-Gonzalez, M.D.; Salto-Gonzalez, R.; Santoyo-Gonzalez, F. Alkyl sulfonyl derivatized PAMAM-G2 dendrimers as nonviral gene delivery vectors with improved transfection efficiencies. *Org. Biomol. Chem.* **2011**, *9*, 851–864. [CrossRef]
21. Li, Z.; Yazaki, R.; Ohshima, T. Chemo-and regioselective direct functional group installation through catalytic hydroxy group selective conjugate addition of amino alcohols to α, β-unsaturated sulfonyl compounds. *Org. Lett.* **2016**, *18*, 3350–3353. [CrossRef] [PubMed]
22. Morales-Sanfrutos, J.; Lopez-Jaramillo, J.; Ortega-Munoz, M.; Megia-Fernandez, A.; Perez-Balderas, F.; Hernandez-Mateo, F.; Santoyo-Gonzalez, F. Vinyl sulfone: A versatile function for simple bioconjugation and immobilization. *Org. Biomol. Chem.* **2010**, *8*, 667–675. [CrossRef] [PubMed]
23. Kantner, T.; Watts, A.G. Characterization of reactions between water-soluble trialkylphosphines and thiol alkylating reagents: Implications for protein-conjugation reactions. *Bioconjugate Chem.* **2016**, *27*, 2400–2406. [CrossRef] [PubMed]
24. Carr, R.V.; Williams, R.V.; Paquette, L.A. Dienophilic properties of phenyl vinyl sulfone and trans-1-(phenylsulfonyl)-2-(trimethylsilyl) ethylene. Their utilization as synthons for ethylene, 1-alkenes, acetylene, and monosubstituted alkynes in the construction of functionalized six-membered rings via [4+2]. pi. cycloaddition methodology. *J. Org. Chem.* **1983**, *48*, 4976–4986.
25. Dalai, S.; Belov, V.N.; Nizamov, S.; Rauch, K.; Finsinger, D.; de Meijere, A. Access to Variously Substituted 5,6,7,8-Tetrahydro-3H-quinazolin-4-ones via Diels–Alder Adducts of Phenyl Vinyl Sulfone to Cyclobutene-Annelated Pyrimidinones. *Eur. J. Org. Chem.* **2006**, *2006*, 2753–2765. [CrossRef]
26. Bull, J.R.; Bischofberger, K. Cycloaddition of phenyl vinyl sulphone to 3-methoxy-16-methylestra-1,3,5(10),14,16-pentaen-17-yl acetate: Synthesis of 14-functional ised 19-norpregnane derivatives. *J. Chem. Soc. Perkin Trans. 1* **1991**, 2859–2865. [CrossRef]

27. Sultan, M.A.; Karama, U. Substituent effects on regioselectivity of the Diels-Alder reactions: Reactions of 10-allyl-1, 8-dichloroanthracene with 2-chloroacrylonitrile, 1-cyanovinyl acetate and phenyl vinyl sulfone. *J. Chem.* **2016**, *2016*. [CrossRef]
28. Iradier, F.; Arrayás, R.G.; Carretero, J.C. Synthesis of medium-sized cyclic amines by selective ring cleavage of sulfonylated bicyclic amines. *Org. Lett.* **2001**, *3*, 2957–2960. [CrossRef]
29. Fustero, S.; Jiménez, D.; Sánchez-Roselló, M.; del Pozo, C. Microwave-assisted tandem cross metathesis intramolecular aza-Michael reaction: An easy entry to cyclic β-amino carbonyl derivatives. *J. Am. Chem. Soc.* **2007**, *129*, 6700–6701. [CrossRef]
30. Kim, S.; Kang, S.; Kim, G.; Lee, Y. Copper-catalyzed aza-Michael addition of aromatic amines or aromatic aza-Heterocycles to α, β-Unsaturated olefins. *J. Org. Chem.* **2016**, *81*, 4048–4057. [CrossRef]
31. Sheldrick, G. *SHELXTL-PC (Version 5.1)*; Siemens analytical instruments Inc.: Madison, WI, USA, 1997.
32. Sheldrick, G.M. A short history of SHELX. *Acta Crystallogr. Sect. A Found. Crystallogr.* **2008**, *64*, 112–122. [CrossRef] [PubMed]
33. Turner, M.; McKinnon, J.; Wolff, S.; Grimwood, D.; Spackman, P.; Jayatilaka, D.; Spackman, M. *Hirshfeld Surfaces and Two-Dimensional Fingerprint Plots Were Generated by Using CrystalExplorer17*; University of Western Australia: Crawley, WA, Australia, 2017.
34. Turner, M.; McKinnon, J.; Wolff, S.; Grimwood, D.; Spackman, P.; Jayatilaka, D.; Spackman, M. *Crystal Explorer17*; University of Western Australia: Crawley, WA, Australia, 2017; Available online: http://hirshfeldsurface.net (accessed on 12 June 2017).
35. Gaussian 09. Revision A.02. Fox Gaussian, D.J. Inc.: Wallingford, CT, USA. 2009. Available online: https://gaussian.com/ (accessed on 26 July 2020).
36. Dennington, R., II; Keith, T.; Millam, J. *GaussView, V. 4.1*; Semichem, Inc.: Shawnee Mission, KS, USA, 2007.